Available online at www.sciencedirect.com
ScienceDirect
Physics Letters B 662 (2008) 245–251
PHYSICS LETTERS B
www.elsevier.com/locate/physletb

Further evidence for $N(1900)P_{13}$ from photoproduction of hyperons

V.A. Nikonov [a,b], A.V. Anisovich [a,b], E. Klempt [a,*], A.V. Sarantsev [a,b], U. Thoma [a]

[a] *Helmholtz-Institut für Strahlen und Kernphysik der Universität Bonn, Germany*
[b] *Petersburg Nuclear Physics Institute, Gatchina, Russia*

Received 1 March 2008; accepted 1 March 2008

Available online 7 March 2008

Editor: M. Doser

Abstract

We report further evidence for $N(1900)P_{13}$ from an analysis of a large variety of photo- and pion-induced reactions, in particular from the new CLAS measurements of double polarization observables for photoproduction of hyperons. The data are consistent with two classes of solutions both requiring contributions from $N(1900)P_{13}$ but giving different $N(1900)P_{13}$ pole positions. $(M - i\Gamma/2) = (1915 \pm 50) - i(90 \pm 25)$ MeV covers both solutions. The small elasticity of 10% or less explains why it was difficult to observe the state in πN elastic scattering.

$N(1900)P_{13}$ is a 2-star resonance which is predicted by symmetric three-quark models. In diquark–quark models, the existence of the state is not expected.

PACS: 11.80.Et; 11.80.Gw; 13.30.-a; 13.30.Ce; 13.30.Eg; 13.60.Le; 14.20.Gk

The flavour structure of baryons and of their resonances is well described in quark models which assume that baryons can be build from three constituent quarks. The spatial and spin-orbital wave functions can be derived using a confinement potential and some residual interactions between constituent quarks. The best known example is the Karl–Isgur model [1], at that time a breakthrough in the understanding of baryons. Later refinements differed by the choice of the residual interactions: Capstick and Isgur continued to use an effective one gluon exchange interaction [2], Plessas and his collaborators used exchanges of Goldstone bosons between the quarks [3], while Löring, Metsch and Petry exploited instanton induced interactions [4]. A group theoretical analysis by Bijker, Iachello and Leviatan gave the same complexity of the spectrum of baryon resonances [5]. Quark models, including a discussion of different decay modes, were reviewed recently by Capstick and Roberts [6].

A common feature of these models is the large number of predicted states: the dynamics of three quarks leads to a rich spectrum, much richer than observed experimentally. The reason for the apparent absence of many predicted states could be that the dynamics of three quark interactions is not understood well enough. It is often assumed for instance that, within the nucleon, two quarks may form a diquark of defined spin and isospin, and that the diquark is not excited. There is a long discussion on the nature and relevance of the diquark concept; we quote here a few recent papers [7–10]. Applied to baryon spectroscopy, the diquark model helps to solve the problem of the *missing baryon resonances*. Santopinto, e.g., calculated the N^* and Δ^* excitation spectrum [11] with the assumption that the baryon is made up from a point-like diquark and a quark. The results match data perfectly, provided N^*- and Δ^*-resonances are omitted from the comparison that have an one- or two-star PDG [12] ranking only.

Of course, there is also the possibility that symmetric quark models treating all three quarks on the same footing are right, and that the large number of predicted but unobserved states reflects an experimental problem. In the region between 1900 and 2000 MeV, there are 3 two-star resonances, $N(1900)P_{13}$, $N(2000)F_{15}$, $N(1990)F_{17}$. According to diquark models, these states should not exist but they are firmly predicted in symmetric three-quark models. An independent confirmation of the states is therefore highly desirable.

* Corresponding author.
E-mail address: klempt@hiskp.uni-bonn.de (E. Klempt).

0370-2693/$ – see front matter
doi:10.1016/j.physletb.2008.03.004

For long time, the main source of information on N^* and Δ^* resonances was derived from pion nucleon elastic scattering. If a resonance couples weakly to this channel, it could thus escape identification. This effect may be the reason for the non-observation of the *missing resonances* or for the weak evidence with which they are observed. Important information is hence expected from experiments studying photoproduction of resonances off nucleons, decaying into complex final states. Such experiments are being carried out at several places. In this Letter we report on further evidence for the $N(1900)P_{13}$, derived from photoproduction, in particular from recent CLAS data on the spin transfer coefficients C_x and C_z from circularly polarized photons to final-state hyperons in the reaction $\gamma p \to \Lambda K^+$ and ΣK^+ [13].

The analysis of photoproduction data is not straightforward. Due to the spin of the initial particles and of the final-state baryon, an unambiguous solution cannot be obtained without polarization observables. Moreover, even in the simplest case of single meson photoproduction a 'complete' experiment from which the full amplitude can be constructed in an energy independent analysis requires the measurements of at least 8 observables [14]. Not only single polarization observables are required but also double polarization variables need to be measured. Photoproduction of hyperons is very well suited to measure double polarization observables since the self-analyzing decay of the hyperon provides access to the hyperon 'induced' polarization, and only one further observable needs to be determined, e.g., by using a polarized photon beam.

Recently, the CLAS Collaboration measured the spin transfer coefficients C_x and C_z from circularly polarized photons to final-state hyperons in the reactions $\gamma p \to \Lambda K^+$ and $\gamma p \to \Sigma^0 K^+$, in the invariant mass region from threshold to $W = 2.454$ GeV [13]. These measurements have yielded the first data expected from a series of double polarization photoproduction experiments which are presently planned and carried out at Bonn, Grenoble, JLab, and Mainz. Even though the new CLAS data provide an important step into the direction of a complete experiment, we are still far from being able to reconstruct fully complex amplitudes in a model independent way. An alternative approach is therefore to include many reactions in a coupled channel analysis. This direction is followed by EBAC, the JLab Excited Baryon Analysis Center [15], by the Giessen group [16] and by the Bonn–Gatchina group [17,18].

The main input into the new analysis presented here are the new data on hyperon photoproduction [13] in combination with the analysis of a large number of other reactions. It will be shown that the data can be described well under an assumption that a further baryon resonance exists in the 1800–2000 MeV mass region which had not been taken into account in our previous fits [19,20]. Identification of the new state with the $N(1900)P_{13}$ is plausible.

Apart from the data on polarization transfer [13], the following data sets were included in the analysis: differential cross sections $\sigma(\gamma p \to \Lambda K^+)$, $\sigma(\gamma p \to \Sigma^0 K^+)$, and $\sigma(\gamma p \to \Sigma^+ K^0)$, recoil polarization, and photon beam asymmetry [21–27]; photoproduction of π^0 and η with measurements of differential cross sections, beam and target asymmetries and recoil polarization from the SAID data base [28–35]. Amplitudes for πN elastic scattering from [36] were included for the low-spin partial waves. The data include about 16 000 data points on two-body reactions; acceptable fits give a total χ^2 of less than 20 000. A more detailed description of the analysis method and comparison of the fit with further data can be found elsewhere [37].

Photoproduction of $2\pi^0$ [38,39] off protons and the recent BNL data on $\pi^- p \to n\pi^0\pi^0$ [40] were also included. These data sets were taken into account in an event-based likelihood fit; at present this data is restricted to the low-mass region ($M < 1.8$ GeV). The data define isobar contributions like $\Delta\pi$ and $N\sigma$ [38] and help to disentangle the properties of the Roper resonance [39] but have little influence on states in the 2 GeV region. The reaction $\gamma p \to p\pi^0\eta$ was included as well; it provides access to ΔP_{33} and ΔD_{33} partial waves which make the largest contributions to the latter reaction [41].

The partial wave analysis presented here is based on relativistically invariant amplitudes constructed from the four-momenta of particles involved in the process [17]. High-spin resonances were described by relativistic multi-channel Breit–Wigner amplitudes, partial waves with low total spin ($J < 5/2$) were described in the framework of the K-matrix/P-vector approach [42]. The S_{11} wave was fitted as 2-pole 5-channel K-matrix (πN, ηN, $K\Lambda$, $K\Sigma$, $\Delta(1232)\pi$); the P_{11}-wave as 3-pole 4-channel K-matrix (πN, $\Delta(1232)\pi$, $N\sigma$, $K\Sigma$) and D_{33} wave as 2-pole 3-channel K-matrix (πN, $\Delta(1232)\pi$, S and D-waves). The P_{13} partial wave is described alternatively by a sum of Breit–Wigner amplitudes or by a 3-pole 8-channel K-matrix. Amplitudes for elastic πN scattering for the S_{11}, P_{11}, D_{33}, and P_{33} partial waves are described using the same K-matrix used for photoproduction. The full parametrization of the S_{11}, P_{11}, and P_{13} partial waves is given in [37].

Resonances may make large contributions to one reaction and smaller contributions to other reactions. This property helps considerably in the identification of resonances and in the determination of their properties. Table 1 lists the strongest contributions in the various reactions which are used in the fits. Further resonances ($N(1675)D_{15}$, $N(1710)P_{11}$, $N(1875)D_{13}$, $N(2000)F_{15}$, $N(2170)D_{13}$, $N(2200)P_{13}$, $\Delta(1620)S_{31}$, $\Delta(1905)F_{35}$) were required to get a good description of the data. Although these states do not contribute strongly to the differential cross sections, they are needed for the description of the polarization variables. In most cases the properties of these states are compatible with the PDG listings. A few additional high-mass resonances were added to describe the intensity. However, spins, parities, masses and widths remained uncertain, and we do not discuss them here.

In the first attempt, the data were fitted using one low-mass Breit–Wigner amplitude to describe the P_{13} wave. A second P_{13} resonance at $M = 2200$ MeV was needed to fit the data on $\gamma p \to p\pi^0\eta$ [41]. No good description of the data was reached. As example, data on C_x, C_z for $\gamma p \to \Lambda K^+$ [13] are compared to the fit in Fig. 1(a). Systematic discrepancies are observed demonstrating the need to introduce further amplitudes. In a second step we added to our solutions, one by one, Breit–Wigner resonances with different quantum num-

bers. The largest improvement was observed introducing a second P_{13} state. The fit optimized at 1885 ± 25 MeV mass and 180 ± 30 MeV width, with improvement of χ^2 for the reactions with two-body final states, $\Delta\chi^2_{2b} = 1540$ where χ^2_{2b} is defined as the (normalized) sum of the χ^2 contributions of all two-body reactions, including their weights (see Eq. (15) in [37]). Adding a S_{11} {or D_{15}} state instead, improved the description by 950 {970} units. Replacing the P_{13} by a P_{11} state resulted in a much smaller improvement, $\Delta\chi^2_{2b} = 205$, probably due to the fact that the fit included already a P_{11} resonance in this mass region. A F_{15} state produced a marginal change in χ^2_{2b} as well; introducing F_{17} and G_{17} did not improve the fit. A resonance with P_{33} quantum numbers state provided a better description of the $\Sigma^0 K^+$ channel and gave some additional freedom to the fit of the ΛK^+ reaction. However, the change in χ^2_{2b} was again smaller by a factor 2 than the one found for a P_{13} state.

Table 1
The four strongest resonant contributions (in decreasing importance) to the reactions included in this analysis. Resonances contributing less than 1% to a reaction are not listed. The contributions are determined for the energy range where data (see text) exist. Note that the ordering of the states is sometimes not well defined: it is, e.g., different for solution 1 (chosen here) and solution 2 discussed below. In some reactions, t- and u-channel exchanges provide a significant contribution to the cross section, too

Reaction	Resonances			
$\gamma p \to N\pi$	$\Delta(1232)P_{33}$	$N(1520)D_{13}$	$N(1680)F_{15}$	$N(1535)S_{11}$
$\gamma p \to p\eta$	$N(1535)S_{11}$	$N(1720)P_{13}$	$N(2070)D_{15}$	$N(1650)S_{11}$
$\gamma p \to p\pi^0\pi^0$	$\Delta(1700)D_{33}$	$N(1520)D_{13}$	$N(1680)F_{15}$	
$\gamma p \to p\pi^0\eta$	$\Delta(1940)D_{33}$	$\Delta(1920)P_{33}$	$N(2200)P_{13}$	$\Delta(1700)D_{33}$
$\gamma p \to \Lambda K^+$	S_{11}-wave	$N(1720)P_{13}$	$N(1900)P_{13}$	$N(1840)P_{11}$
$\gamma p \to \Sigma K$	S_{11}-wave	$N(1900)P_{13}$	$N(1840)P_{11}$	
$\pi^- p \to n\pi^0\pi^0$	$N(1440)P_{11}$	$N(1520)D_{13}$	S_{11}-wave	

Fig. 2 demonstrates the gain in fit quality when a P_{13} state is introduced. The figure shows differential cross section and the beam asymmetry for $\gamma p \to \Lambda K^+$ and $\gamma p \to \Sigma^0 K^+$ in the region of $N(1900)P_{13}$. In particular the $\Sigma^0 K^+$ differential distributions are not reasonably described without introduction of a new resonance. The agreement in these figures can be improved by giving a higher weight to this particular data but on the expense of problems showing up at other places.

In a final step, the P_{13} was introduced as 3-pole 8-channel K-matrix with πN, ηN, $\Delta(1232)\pi$ (P- and F-waves), $N\sigma$, $D_{13}(1520)\pi$ (S-wave), $K\Lambda$, and $K\Sigma$ channels. A satisfactory description of the C_x and C_z distributions was obtained for both, the ΛK^+ (see Fig. 1(b)) and the $\Sigma^0 K^+$ channel (not shown). The inclusion of the $N(1900)P_{13}$ resonance was essential to achieve a good quality of the fit, not only for the new C_x, C_z but also for other data. The χ^2/N_F for the differential

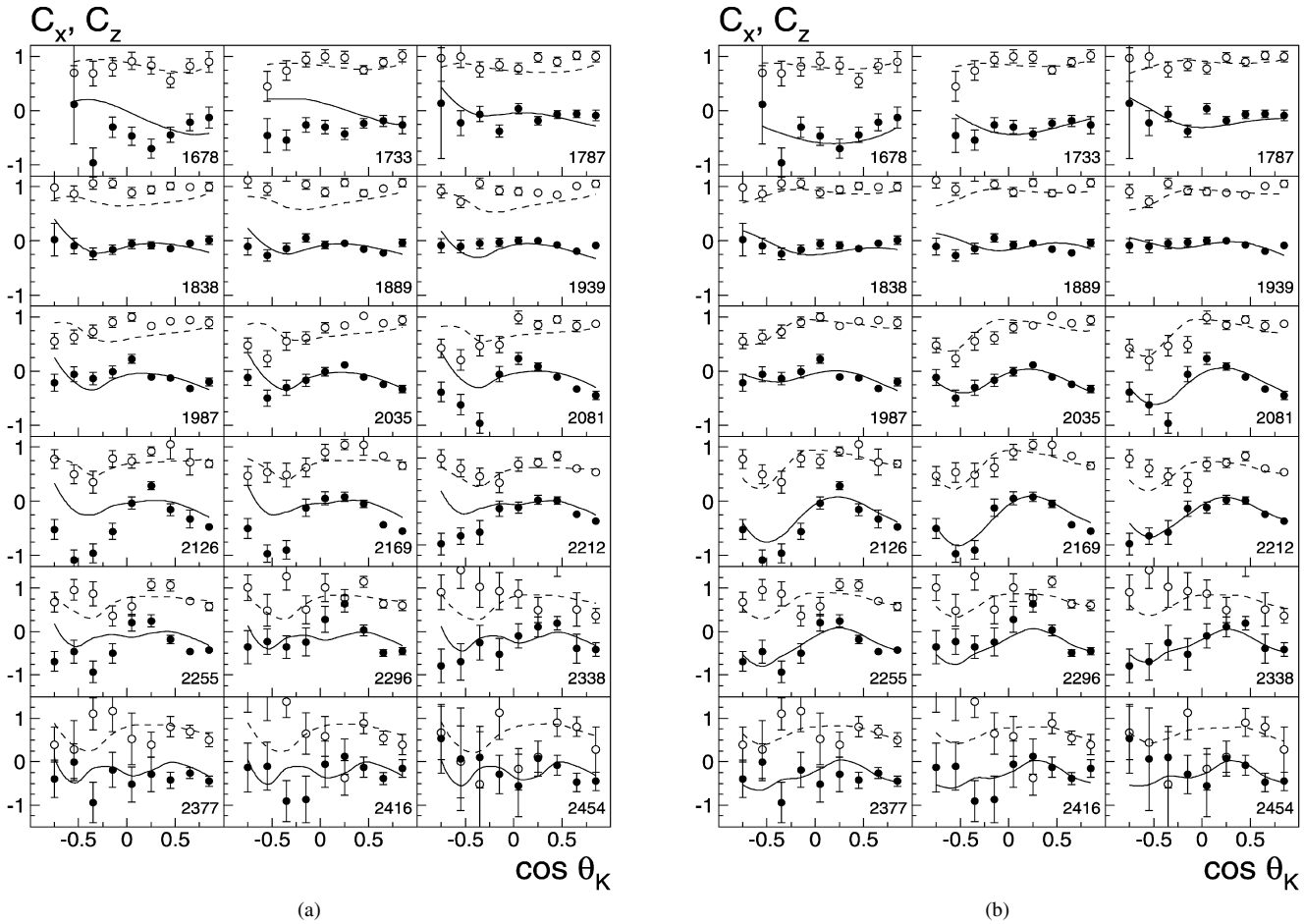

Fig. 1. Double polarization observables C_x (black circle) and C_z (open circle) for $\gamma p \to \Lambda K^+$ [13]. The solid (C_x) and dashed (C_z) curves are our result obtained without (a) and with the $N(1900)P_{13}$ state (b) included in the fit.

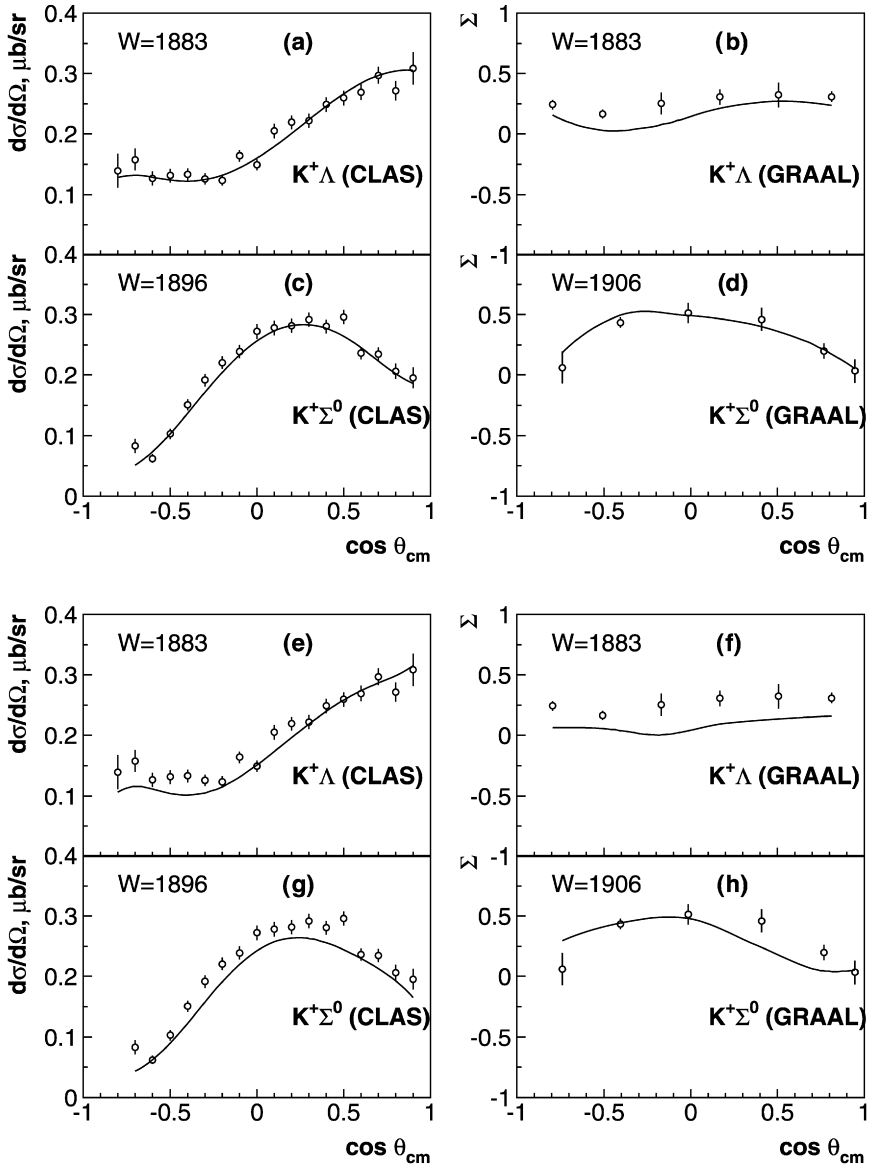

Fig. 2. Differential cross section [13] and beam asymmetry for $\gamma p \to \Lambda K^+$ and $\gamma p \to \Sigma^0 K^+$ in the region of $N(1900)P_{13}$. The solid curves present our best fit with the $N(1900)P_{13}$ state included (subfigures (a)–(d)) or omitted (subfigures (e)–(h)) and all other variables re-optimized.

ΛK^+ ($\Sigma^0 K^+$) cross section reduced from 2.35 to 2.0 (2.4 to 2.1) when the $N(1900)P_{13}$ resonance was introduced. Fig. 1 shows the best fit without (a) and with (b) $N(1900)P_{13}$ included. When the P_{13}-wave was treated as K-matrix, introduction of a third resonance (representing $N(1900)P_{13}$) improved χ^2 for ΛK^+ and ΣK data by 1650 units, a significant number. Overall, the fit proved to be marginally better than the fit using Breit–Wigner amplitudes.

The χ^2 change as a function of the $N(1900)P_{13}$ mass is shown in Fig. 3. The ΛK^+ data exhibit two minima, corresponding to solution 1 and solution 2, discussed below; the ΣK prefer the lower mass for $N(1900)P_{13}$. Note the different definitions of the unweighted χ^2 shown in Fig. 3 and the weighted χ^2_{2b} used in the fits.

The data set used in this analysis, even though comprising nearly all available information, is still not yet sufficient to determine a unique solution. For different start values, the fit can converge to different minima. As a rule, we accepted all fits which gave a reasonable description of all data sets and did not show a significant problem in one of the reactions included. Fits were rejected, when we found that the trend of the data was inconsistent with the fit curve even if the increase in χ^2 in some low-statistics data was counterbalanced by an improved description of some high-statistics data. When the trend of some data was inconsistent with the fit curve, we increased the weight of that data until reasonable consistency was obtained. The variety of different solutions was used to define the final errors.

All solutions considered from now on include the P_{13} state and give a reasonable description of all data. However the contributions of the different isobars to the fitted channels are not uniquely defined. We observed two classes of solutions which we call the first and second solution. Both solutions yield a similar overall χ^2_{2b}. In the first solution, the pole of the P_{13} partial wave is situated at about 1870 MeV and provides a notice-

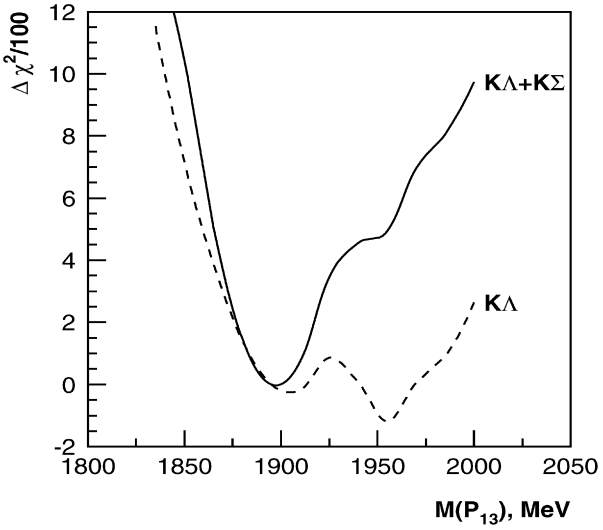

Fig. 3. The change of χ^2 for the fit to photoproduction of ΛK^+ and ΣK as a function of the assumed $N(1900)P_{13}$ mass.

able contribution to the ΛK^+ and $\Sigma^0 K^+$ total cross sections. It is responsible for the double peak structure in the ΛK^+ total cross section and helps to describe the peak in the $\Sigma^0 K^+$ total cross section. In the $\gamma p \to K^0 \Sigma^+$ channel, the contribution of the P_{13} state has a similar strength as the $N(1840)P_{11}$ state reported in [20] where the possible presence of an additional P_{13} state was already discussed even though it could not yet be identified unambiguously. In this first solution, the P_{11} pole moved to 1880 MeV and became broader. Interference of this pole with the pole at the region 1700 MeV generated a comparatively narrow structure in the $\gamma p \to K^0 \Sigma^+$ total cross section.

In the second type of the solutions (the second solution) the P_{13} pole is found at about 1950 MeV. It provides rather small contributions to the ΛK^+ and $\Sigma^0 K^+$ total cross sections while the main contribution to the $\gamma p \to K^0 \Sigma^+$ cross section now comes from a P_{11} state. The new impact of the P_{13} state is an improvement of the description of double polarization variables due to interferences. The data are described reasonably well in both solutions, including those on C_x and C_z except perhaps in two slices in the 2.15 GeV mass region (see Fig. 1 for solution 1).

A few regions show small but systematic deviations. The first solution does not describe well the ΛK^+ recoil polarization at backward angles in the 1700 MeV region. The description can be improved by the introduction of an additional state in the 1800 MeV region, with quantum numbers P_{33}, D_{15} or S_{11}. In the latter case, the data might demand a more sophisticated parameterization of the S_{11} wave by, for example, taking into account the $\rho(770)N$ threshold. Thus it is not clear if an additional resonance is really needed. Furthermore, we are not sure that, with the present quality of the data, these additional states or/and threshold effects can be identified with reasonable confidence. We therefore decided to postpone attempts to identify weaker signals until new data are available. The main result of the present analysis is that a satisfactory description of the

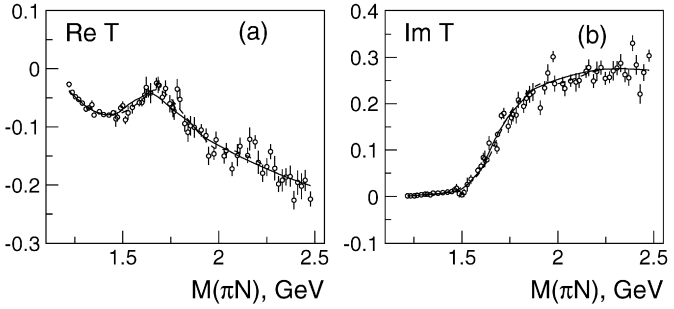

Fig. 4. Real (a) and imaginary (b) part of the $\pi N P_{13}$ elastic scattering amplitude [36] and the result of our fit. Solution 1: solid curve, solution 2: dashed curve.

fitted data can be obtained by introduction of just one new resonance, a relatively narrow P_{13} state at about 1885 MeV or 1975 MeV.

The new P_{13} state also improves the description of the $\gamma p \to K^+ \Sigma^0$ reaction, even though its effect is much less visible here. The double polarization data in this channel were already described reasonably well in our previous analysis (see the figures in [13]); and a slight readjustment of the fit parameters gave a good representation of the data. The main contribution to $\gamma p \to K^+ \Sigma^0$ data is now due to K-exchange. In [20], the larger contribution was assigned to K^* exchange. A dominance of K exchange explains naturally the small $\gamma p \to K^0 \Sigma^+$ cross section which is forbidden for K exchange. The P_{13} partial wave provides a moderate contribution to the cross section but helps to achieve a good fit.

To check whether elastic data are compatible with the new state, we introduced it as an additional K-matrix pole and fitted the $\pi N \to \pi N P_{13}$ partial wave for invariant masses up to 2.4 GeV. A satisfactory description of all fitted observables was obtained; as example we show the elastic scattering data in Fig. 4.

Most masses and widths obtained in the fits are compatible with the numbers given in [19,20]. Here we comment only on the P_{13} partial wave. The parameters of the two lowest P_{13} poles are given in Table 2. For both solutions, the first P_{13} state was found to be a rather broad state. Most previous analyses gave much narrower Breit–Wigner widths [12].

However, Manley and Saleski [43], the only earlier analysis which includes $N2\pi$ decays, reported a width of 380 ± 180 MeV. The most recent $\pi N \to N\pi$ plus $N\eta$ analysis of Arndt et al. [36] gave a pole position at $M = 1666$, $\Gamma = 355$ MeV with no error, not too far from our pole position at $M = 1640 \pm 80$, $\Gamma = 480 \pm 60$ or (2nd solution) $M = 1630 \pm 80$, $\Gamma = 440 \pm 60$. Only, the Breit–Wigner widths differ substantially. Arndt et al. gave $M = 1763.8 \pm 4.6$, $\Gamma = 210 \pm 22$ MeV while we find 1800 ± 100 (1780 ± 80) MeV mass and 700 ± 100 (680 ± 80) MeV width where the numbers correspond to the first, those in parentheses to the second solution.

The difference in the Breit–Wigner width could indicate a problem. Attempts to find solutions with a narrower $N(1720)P_{11}$ (with widths in the 150–250 MeV range) failed. Yet, Breit–Wigner parameters are certainly model dependent. The Breit–

Table 2
Properties of the two lowest P_{13} resonances for both solutions. The masses, widths are given in MeV, the branching ratios in % and helicity couplings in 10^{-3} GeV$^{-1/2}$. The helicity couplings and phases were calculated as residues in the pole position

	Solution 1		Solution 2	
M_{pole}	1640 ± 80	1870 ± 15	1630 ± 60	1960 ± 15
$\Gamma_{\text{tot}}^{\text{pole}}$	480 ± 80	170 ± 30	440 ± 60	195 ± 25
$A_{1/2}$	140 ± 80	$-(10 \pm 15)$	160 ± 40	$-(18 \pm 8)$
$\varphi_{1/2}$	$-(10 \pm 15)^\circ$	–	$(10 \pm 15)^\circ$	$-(40 \pm 15)^\circ$
$A_{3/2}$	150 ± 80	$-(40 \pm 15)$	70 ± 30	$-(35 \pm 12)$
$\varphi_{3/2}$	$-(40 \pm 30)^\circ$	$(30 \pm 25)^\circ$	$(0 \pm 20)^\circ$	$-(40 \pm 15)^\circ$
$\text{Br}_{N\pi}$	8 ± 4	5 ± 3	18 ± 5	6 ± 3
$\text{Br}_{N\eta}$	14 ± 4	20 ± 8	10 ± 2	15 ± 3
$\text{Br}_{K\Lambda}$	16 ± 6	15 ± 5	7 ± 2	12 ± 3
$\text{Br}_{K\Sigma}$	<2	22 ± 8	<1	8 ± 2
$\text{Br}_{\Delta\pi(P)}$	54 ± 10		36 ± 6	
$\text{Br}_{\Delta\pi(F)}$	2 ± 2		18 ± 5	
$\text{Br}_{D_{13}\pi}$	2 ± 2		5 ± 3	
$\text{Br}_{N\sigma}$	4 ± 2		4 ± 2	
Br_{Add}	<2	38 ± 12	2 ± 2	60 ± 6

Wigner parameters we quote are derived using the Flatte formula: the amplitude is forced to have exactly the same pole position as the T-matrix derived from a K-matrix fit. The state couples strongly to $\Delta(1232)\pi$ and, in the second solution, also to the $D_{13}(1520)\pi$ channel with large couplings but moderate branching ratio. This effect requires a large fitted width even though the observed width remains reasonable. We have inspected the intensity distribution of the P_{13} amplitude in the $N\pi$ and $N\eta$ channel and found peak positions at 1680 and 1700 MeV, and observable widths (full width at half maximum) of 250 and 270 MeV, respectively. The large width is thus a consequence of the complex pole structure of $N(1720)P_{11}$. The $D_{13}(1520)\pi$ threshold is close to the resonance mass and creates a double pole structure. The two poles are hidden under a Riemann sheet created by a cut at the $D_{13}(1520)\pi$ threshold; the closest physical region for them is situated above the $D_{13}(1520)\pi$ threshold. The situation is similar to the $a_0(980)$ case where its large coupling to $K\bar{K}$ creates a narrow structure in the $\pi\eta$ mass distribution.

The pole structure renders the definition of helicity amplitudes and of decay partial widths complicated; here these quantities are calculated in a procedure described in [37] as residues of the poles of the scattering matrix (T-matrix).

The pole of the second P_{13} state is situated in the region 1850–2000 MeV; it has a smaller coupling to the πN channel. In the first class of solutions, this coupling can be a positive or a negative value. The helicity couplings are, however, defined under the assumption that the coupling to the πN channel is a positive number. Thus the sign of the helicity coupling is ambiguous. In the analysis [19], only one P_{13} state below 2.0 GeV was needed to describe the data. This state was found to be rather broad and to couple to the ηn channel with branching ratio 8–12%. The present analysis reproduces the P_{13} partial wave in the $\gamma p \to \eta N$ reaction even though the broad structure is produced now due to an interference of two poles.

In summary, we have analyzed the new CLAS data on spin transfer from circularly polarized photons to Λ and Σ hyperons in the final state. Included in the analysis are other data on photo- and pion-induced reactions. One additional resonance (compared to previous fits) is needed to achieve a good description of all data. Quantum numbers P_{13} are preferred. In spite of the large data set which includes differential distributions, beam, target and recoil asymmetries, and some double polarization data, no unique solution was found. But all solutions require a P_{13} state. The two classes of solutions from this analysis optimize for masses (and widths) of 1870 (170) or 1960 (195) MeV, respectively. We assign mass and width of $M = 1915 \pm 60$ MeV and $\Gamma = 180 \pm 40$ MeV which covers the large majority of all solutions we have obtained. The elastic widths is about 2–9%, the branching fraction to ΛK^+, 5–15%.

Clearly, this is a first step to make $N(1900)P_{13}$ a four-star accepted resonance. Needed are more polarization data, in particular further double polarization data, and refined analysis techniques taking into account additional singularities due to final state interactions in complex final states like $N\pi\pi$ [15]. Because of the stability of the need to introduce a $N(1900)P_{13}$ resonance in the fit when the fit hypothesis is changed we are, however, confident that the resonance will survive further scrutiny tests.

The Particle Data Group lists two entries for $N(1900)P_{13}$; Manley and Saleski find mass and width of 1879 ± 17 (498 ± 78) MeV, the elastic widths is determined to 0.26 ± 0.06 [43]. Penner and Mosel find 1951 ± 53 (622 ± 42) MeV and an elastic width of 0.16 ± 0.02 [44,45]. The ΛK^+ branching fraction was determined to $2.4 \pm 0.3\%$ by Shklyar and Mosel [16].

Even though there are considerable inconsistencies between the four analyses, it seems most likely that the observations are traces of one resonance. Given its mass and quantum numbers, it can be ascribed to a quark model state which requires excitation of both oscillators in the 3-body system. The $N(1900)P_{13}$ is unlikely to be explainable in a picture where a quark is bound by a "good" diquark.

Acknowledgements

The work was supported by the DFG within the SFB/TR16 and by a FFE grant of the Research Center Jülich. U. Thoma thanks for an Emmy Noether grant from the DFG. A. Sarantsev gratefully acknowledges the support from Russian Science Support Foundation. This work is also supported by Russian Foundation for Basic Research 07-02-01196-a and Russian State Grant Scientific School 5788.2006.2.

References

[1] N. Isgur, G. Karl, Phys. Rev. D 19 (1979) 2653;
N. Isgur, G. Karl, Phys. Rev. D 23 (1981) 817, Erratum.
[2] S. Capstick, N. Isgur, Phys. Rev. D 34 (1986) 2809.
[3] L.Y. Glozman, et al., Phys. Rev. D 58 (1998) 094030.
[4] U. Löring, et al., Eur. Phys. J. A 10 (2001) 395;
U. Löring, et al., Eur. Phys. J. A 10 (2001) 447.
[5] R. Bijker, F. Iachello, A. Leviatan, Ann. Phys. 236 (1994) 69.
[6] S. Capstick, W. Roberts, Prog. Part. Nucl. Phys. 45 (2000) S241.

[7] M. Anselmino, E. Predazzi, S. Ekelin, S. Fredriksson, D.B. Lichtenberg, Rev. Mod. Phys. 65 (1993) 1199.
[8] M. Kirchbach, M. Moshinsky, Yu.F. Smirnov, Phys. Rev. D 64 (2001) 114005.
[9] R.L. Jaffe, F. Wilczek, Phys. Rev. Lett. 91 (2003) 232003.
[10] R.L. Jaffe, Phys. Rep. 409 (2005) 1, Nucl. Phys. B (Proc. Suppl.) 142 (2005) 343.
[11] E. Santopinto, Phys. Rev. C 72 (2005) 022201.
[12] W.M. Yao, et al., Particle Data Group, J. Phys. G 33 (2006) 1.
[13] R. Bradford, et al., CLAS Collaboration, Phys. Rev. C 75 (2007) 035205.
[14] W.T. Chiang, F. Tabakin, Phys. Rev. C 55 (1997) 2054.
[15] A. Matsuyama, T. Sato, T.S. Lee, Phys. Rep. 439 (2007) 193.
[16] V. Shklyar, H. Lenske, U. Mosel, Phys. Rev. C 72 (2005) 015210.
[17] A.V. Anisovich, et al., Eur. Phys. J. A 24 (2005) 111.
[18] A.V. Anisovich, A.V. Sarantsev, Eur. Phys. J. A 30 (2006) 427.
[19] A.V. Anisovich, et al., Eur. Phys. J. A 25 (2005) 427.
[20] A.V. Sarantsev, et al., Eur. Phys. J. A 25 (2005) 441.
[21] K.H. Glander, et al., Eur. Phys. J. A 19 (2004) 251.
[22] J.W.C. McNabb, et al., Phys. Rev. C 69 (2004) 042201.
[23] R.G.T. Zegers, et al., Phys. Rev. Lett. 91 (2003) 092001.
[24] R. Lawall, et al., Eur. Phys. J. A 24 (2005) 275.
[25] R. Bradford, et al., Phys. Rev. C 73 (2006) 035202.
[26] A. Lleres, et al., Eur. Phys. J. A 31 (2007) 79.
[27] R. Castelijns, et al., nucl-ex/0702033.
[28] R.A. Arndt, et al., http://gwdac.phys.gwu.edu.
[29] A.A. Belyaev, et al., Nucl. Phys. B 213 (1983) 201;
R. Beck, et al., Phys. Rev. Lett. 78 (1997) 606;
D. Rebreyend, et al., Nucl. Phys. A 663 (2000) 436.
[30] K.H. Althoff, et al., Z. Phys. C 18 (1983) 199;
E.J. Durwen, BONN-IR-80-7 (1980);
K. Buechler, et al., Nucl. Phys. A 570 (1994) 580.
[31] B. Krusche, et al., Phys. Rev. Lett. 74 (1995) 3736.
[32] J. Ajaka, et al., Phys. Rev. Lett. 81 (1998) 1797.
[33] O. Bartholomy, et al., Phys. Rev. Lett. 94 (2005) 012003.
[34] V. Crede, et al., Phys. Rev. Lett. 94 (2005) 012004.
[35] O. Bartalini, et al., Eur. Phys. J. A 26 (2005) 399.
[36] R.A. Arndt, W.J. Briscoe, I.I. Strakovsky, R.L. Workman, Phys. Rev. C 74 (2006) 045205.
[37] A.V. Anisovich, V. Kleber, E. Klempt, V.A. Nikonov, A.V. Sarantsev, U. Thoma, arXiv: 0707.3596.
[38] U. Thoma, et al., arXiv: 0707.3592.
[39] A.V. Sarantsev, et al., arXiv: 0707.3591.
[40] S. Prakhov, et al., Phys. Rev. C 69 (2004) 045202.
[41] I. Horn, et al., arXiv: 0711.1138.
[42] I.J.R. Aitchison, Nucl. Phys. A 189 (1972) 417.
[43] D.M. Manley, E.M. Saleski, Phys. Rev. D 45 (1992) 4002.
[44] G. Penner, U. Mosel, Phys. Rev. C 66 (2002) 055211.
[45] G. Penner, U. Mosel, Phys. Rev. C 66 (2002) 055212.